Macromolecules

pubs.acs.org/Macromolecules

Article

Sustainable and Eco-Compatible Copolyesters with Applicable Properties: Controlled One-Pot Synthesis and Chemically Closed-Loop Recycling

Zheng-He Yang,[†] Xue-Ping Ou-Yang,[†] Si-Chong Chen, Gang Wu,* and Yu-Zhong Wang*

Cite This: *Macromolecules* 2025, 58, 4183−4193

Read Online

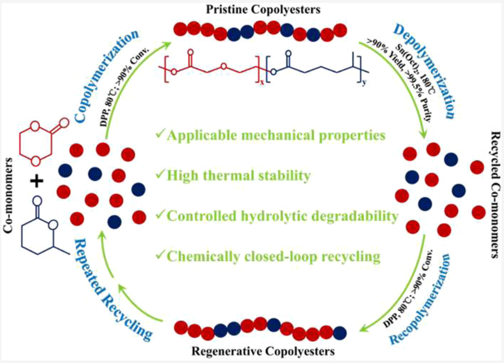

ABSTRACT: The vast usage of conventionally nondegradable petrochemical-based plastics and their improper disposal have posed depletion of energy, shortage of resources, and some environmental concerns, which impels to develop new eco-compatible and sustainable alternatives with considerable performances and economic benefits. Herein, we report a class of novel degradable and chemically recyclable copolyesters with desired and controlled properties. These copolyesters with a near-random sequence structure are rationally designed and controllably synthesized by one-pot bulk ring-opening polymerization (ROP) of *p*-dioxanone and δ-hexanolactone (HL) using a commercial organic catalyst. The effect of the random sequence on the properties of copolyesters is investigated systematically. It is found that the introduction of a small amount of HL monomer to make a slight degree of random in copolyesters can effectively balance their comprehensive performance. Significantly, a good trade-off of tensile strength and elongation-at-break of the copolyesters, being comparable to general plastics and those of most widely used degradable plastics, is realized. In addition, the copolyesters posess excellent thermal stability (a decomposing temperature of approximately 300 °C) and delayed hydrolytic degradability that meets the demands of melt-processing and practical applications. Moreover, not only is direct thermal depolymerization of the copolyesters to comonomers achieved with a yield of exceed 95% and purity of up to 99.7% but also the repolymerization of recycled comonomers to prepare the regenerative copolyesters with nearly identical structures and properties to the initial copolyesters is successfully implemented, solidly demonstrating the chemically closed-loop recycling of this copolyester for the first time.

■ INTRODUCTION

Plastics derived from finite fossil feedstocks have been widely used in all aspects of daily lives, such as packaging, construction, electronics, and vehicle, because of their low cost, lightweight, good processability, as well as versatile mechanical properties. However, due to high chemical stability of most of them (for example, polyolefin and aromatic polyester), it is predicted that 11 billion metric tons of plastics after service life will accumulate in the environment and landfills by 2025,[1] and worse still, their degradation would take hundreds or even thousands of years,[2] causing severe environmental and health concerns.[3−5]

To address these issues, great efforts have been made including the development of eco-compatible alternatives (such as biodegradable polymers) or the mechanical/chemical recycling of conventionally nondegradable plastics.[6−10] However, most biodegradable polymers with applicable properties, such as polylactide (PLA) and poly(3-hydroxybutyrate) (PHB), which are from the polymerization of expensive monomers, not only decompose to low-value products (e.g., carbon dioxide and water, which are difficult to use directly as chemical raw materials) in artificial environments (such as compost), resulting in waste of resources, but also do not undergo efficient degradation in natural environments (such as seawater), which bring potential environmental risk.[11] On the other hand, mechanical recycling of conventional non-degradable plastics frequently leads to obtain the non-degradable recycled products with severely deteriorative performance and typically results in substantial loss of quality accompanying with emission of potentially harmful fragments (so-called microplastics), which is unsustainable and downgraded approach.[12] Therefore, it is highly desirable to develop an ideal plastic with both degradability and chemical recyclability that can not only completely degrade when discarded into various natural environments but also depolymerize into its constituent monomers for repolymerization after collection.[13,14] This ideal plastic is both sustainable,

Received: October 11, 2024
Revised: April 2, 2025
Accepted: April 4, 2025
Published: April 11, 2025

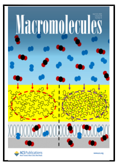

https://doi.org/10.1021/acs.macromol.4c02498

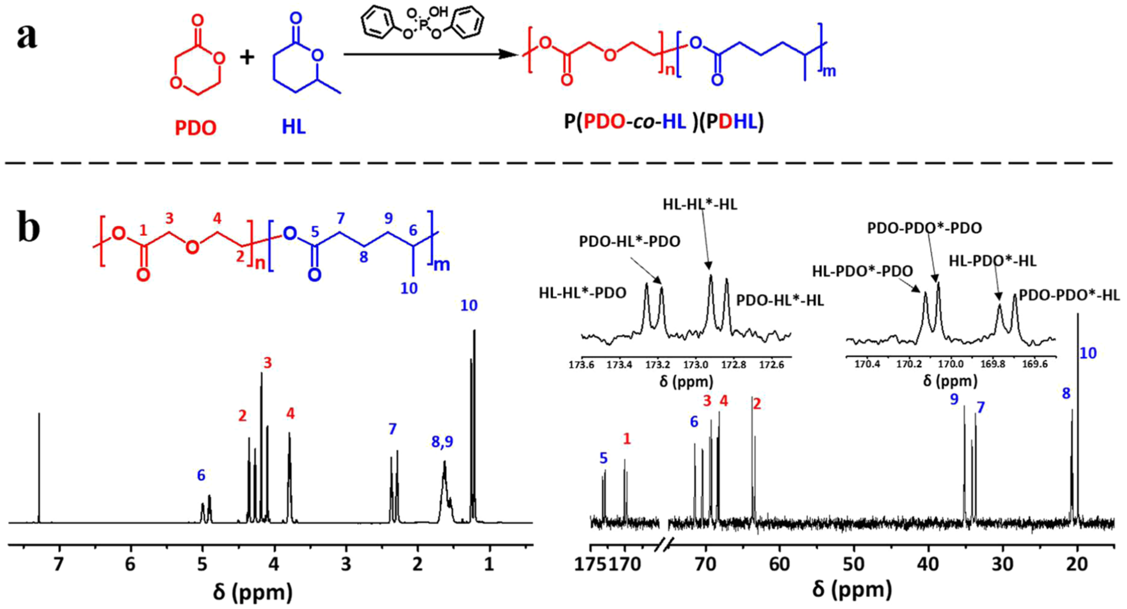

Figure 1. (a) Copolymerization of PDO with HL monomer. (b) ^{1}H NMR spectrum (left) and ^{13}C NMR spectrum (right) of copolymer PDHL$_{50\%}$.

helping to preserve finite natural resources, and eco-compatible, addressing end-of-life issues.

It is essential for developing the degradable and chemically recyclable plastic to design and synthesize polymer. Recently some degradable and chemically recyclable polymers have been exploited, such as ring-opening metathesis-based polymers,[15] polycarbonates,[16−18] and aliphatic polyesters.[19−26] Although these reported polymer systems have presented significant merits, the development of more advanced degradable and chemically recyclable plastics with easily accessible monomers and applicable comprehensive properties (e.g., thermal stability and mechanical property) that can be efficiently prepared by controlled polymerization, completely degraded in natural environments, and facilely depolymerized to initial monomers with high yield and purity under mild conditions is still a great challenge.[27−29]

To meet this challenge, researchers need to analyze the balance between polymerization and degradation in terms of the thermodynamic properties of polymers. In the description of equilibrium thermodynamics by Dainton's equation, there is a critical temperature in ring-opening polymerization (ROP) at which the polymerization is at equilibrium, namely the so-called ceiling temperature (T_c).[30] T_c can be used to estimate the reaction tendency of the equilibrium reaction between ROP and ring-closing depolymerization.[31] Polymers with a high T_c, typically, such as PLA and PCL, are easy to polymerize but hard to depolymerize. They usually present low depolymerization selectivity, which is mainly manifested in the complex products obtained by the depolymerization of PCL and the existence of oligomers and dimers, whereas PLA is easy to racemize during the depolymerization.[14] Poly(γ-butyrolactone) (γ-BL) is a typical example of low T_c, its depolymerization occurs easily under mild conditions, but its polymerization usually needs to be conducted at harsh conditions, such as low temperature, high pressure, or expensive catalysts, which is not conducive to an implementation of industrialization.[32] In comparison, poly(p-dioxanone) (PPDO) with a moderate T_c is easily synthesized by ROP of p-dioxanone (PDO) and has satisfactory mechanical properties, good biodegradability and biocompatibility, as well as high-efficiency depolymerization to PDO monomer.[33,34] Therefore, the development of PPDO-based aliphatic copolyesters with tunable performance or diverse functionality not only has the potential to expand their applications[35−40] but it is also of great significance to solve the problems caused by plastics.

In this work, a biosourced lactone monomer with a moderate T_c, i.e., methyl substituted pentanolactone (δ-hexanolactone, HL), was introduced in PPDO to obtain the PPDO-based copolyesters with a near-random sequence structure through one-pot bulk ring-opening copolymerization. In order to better maintain the advantages of PPDO, we rationally designed and controllably synthesized degradable and chemically recyclable aliphatic copolyesters with a low-level degree of random in PPDO segments, as potentially sustainable and eco-compatible plastics with applicable properties. The copolyesters exhibit good mechanical properties with a trade-off of tensile strength and elongation-at-break (a tensile strength at break of 25 MPa and an elongation-at-break of 246%), which are comparable to the two general plastics poly(ethylene terephthalate) (PET) and low-density polyethylene (LDPE) as well as two most widely used degradable plastics PLA and poly(3-hydroxybutyrate) (PHB), as shown in Table S1.[38−40] Significantly, the copolyesters possess an excellent thermal stability (a decomposing temperature of approximately 300 °C) that meets the demand of melt-processing, and under the guidance of our in depth pyrolysis research, they can almost completely depolymerize into the corresponding comonomers with a yield of over 96% and a purity of high to 99.7% in the presence of a commercial catalyst (stannous octanoate, about 1 wt %) at 180 °C under vacuum pressure for several hours. Moreover, the recovered comonomers can be repolymerized directly to produce well-defined copolyesters with almost the same structures and properties as initial copolyesters, demonstrating that the closed-loop recycling of this copolyester was realized for the first time. In addition, the copolyesters show a controlled hydrolytic degradability, which will balance between degradability and durability in the water environment.

Table 1. Results of Homopolymerization and Copolymerization of PDO with HL[a]

sample	HL content in feed[b] (%)	conv.$_{HL}$ (%)	conv.$_{PDO}$ (%)	F_{HL}[c] (%)	M_w (kg/mol)	D	[η] (dg/L)
PPDO	0	N. A	93.5	N. A	77.3	1.79	1.10
PDHL$_{4.8\%}$	5	91.5	93.3	4.8	65.8	1.77	1.09
PDHL$_{8.9\%}$	10	90.8	94.6	8.9	56.5	1.76	1.09
PDHL$_{13.1\%}$	15	92.7	94.3	13.1	49.8	1.70	1.01
PDHL$_{17.1\%}$	20	92.3	93.1	17.1	48.5	1.74	1.01
PHL	100	90.9	N. A	100	25.2	1.52	N. A

[a] DPP as catalyst and $Ph(CH_2OH)_2$ as initiator, $[M]_0$:Cat:I = 1000:4:1, reaction at 80 °C for 36 h. [b] Molar percentage of the HL monomer in feed. [c] The amount of HL incorporation of copolymers measured by ^1H NMR.

Table 2. Thermal properties of the different copolymers together with PPDO and PHL homopolymers

sample	$T_{5\%}$ (°C)	T_{max} (°C)	F_{HL} (%)	T_m[a] (°C)	ΔH_m[a] (J/g)	T_g (°C)	$T_{cryst.}$[b] (°C)	$\chi_{c,PPDO}$[e] (%)	T_m[f] (°C)	ΔH_m[f] (J/g)
PPDO	306	385	0	108.9	81.5	−8.4	69.8[c]	58	109.1	70.9
PDHL$_{4.8\%}$	265	368	4.8	100.4	63.4	−11.7	49.2[d]	47	99.9	58.0
PDHL$_{8.9\%}$	253	369	8.9	92.8	51.3	−12.8	58.4[c]	40	93.2	38.5
PDHL$_{13.1\%}$	273	372	13.1	84.3	51.6	−14.7	N. A	42	85.7	1.5
PDHL$_{17.1\%}$	296	364	17.1	77.0	46.3	−15.5	N. A	40	N. A	N. A
PHL	250	344	100	53.9	16.6	−36.7	N. A	N. A	N. A	N. A

[a] Recorded according to the first heating scans of the DSC curves, the samples melt at 120 °C and annealed to room temperature before DSC tests. [b] Represented the crystallization temperature of the sample. [c] Recorded according to the cooling scan. [d] Recorded according to the second heating scans. [e] Degree of crystallinity of PPDO, $\chi_{c,PPDO}$ (%) = 100 × $\Delta H_m/\Delta H_m^0 \times 1/\varphi$, φ is the weight fraction of PDO, ΔH_m^0 = 141.2 J/g.[45] [f] Recorded according to the second heating scans.

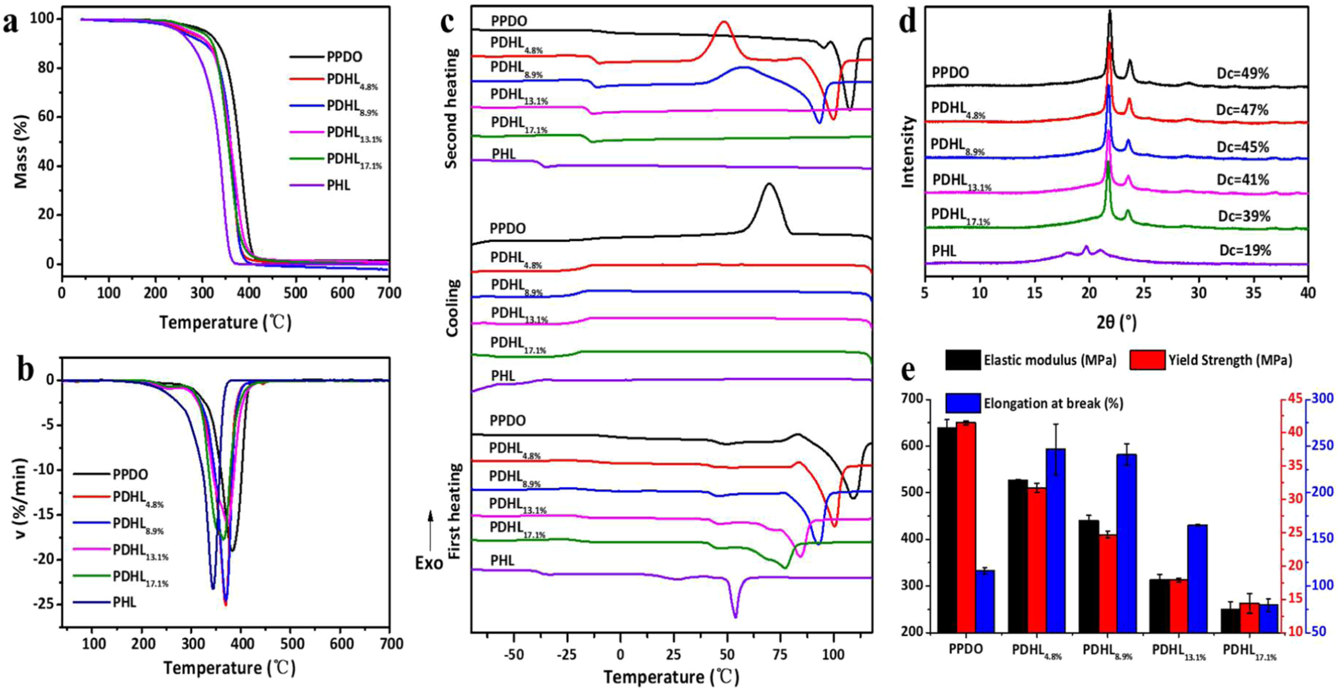

Figure 2. Thermal properties and crystallization behavior of the different copolymers and homopolymers: (a) TGA curves, (b) DTG curves, (c) DSC curves, and (d) XRD curves. (e) Mechanical properties of PPDO homopolymer and the different copolymers.

■ RESULTS AND DISCUSSION

Synthesis and Microstructural Analysis. The catalysts with high catalytic activity for both *p*-dioxanone (PDO) and *δ*-hexanolactone (HL) were screened to synthesize copolymers of PDO and HL (PDHL) with designated composition and high atomic economy. Stannous octanoate ($Sn(Oct)_2$) as a metal-based catalyst is the most frequently used catalyst for ring-opening polymerization (ROP) of PDO;[33] meanwhile, diphenyl phosphate (DPP) as an organic acid catalyst is reported in ROP of *δ*-valerolactone (VL) and its derivatives.[23,41] Accordingly, the homopolymerization of PDO and HL as well as their copolymerization catalyzed by either $Sn(Oct)_2$ or DPP were investigated, and the results are summarized in Table S2. As a control, PDO and HL were first homopolymerized using the $Sn(Oct)_2$/DPP-1,4-butanediol (BDO) catalyst-initiator system. It can be found that $Sn(Oct)_2$ possesses an extremely high catalytic activity for PDO with 99% conversion (sample PPDO-1) but is not applicable for catalyzing the ROP of HL (sample PHL-1). When the ratio of monomer to $Sn(Oct)_2$ was 500:1 without an extra initiator

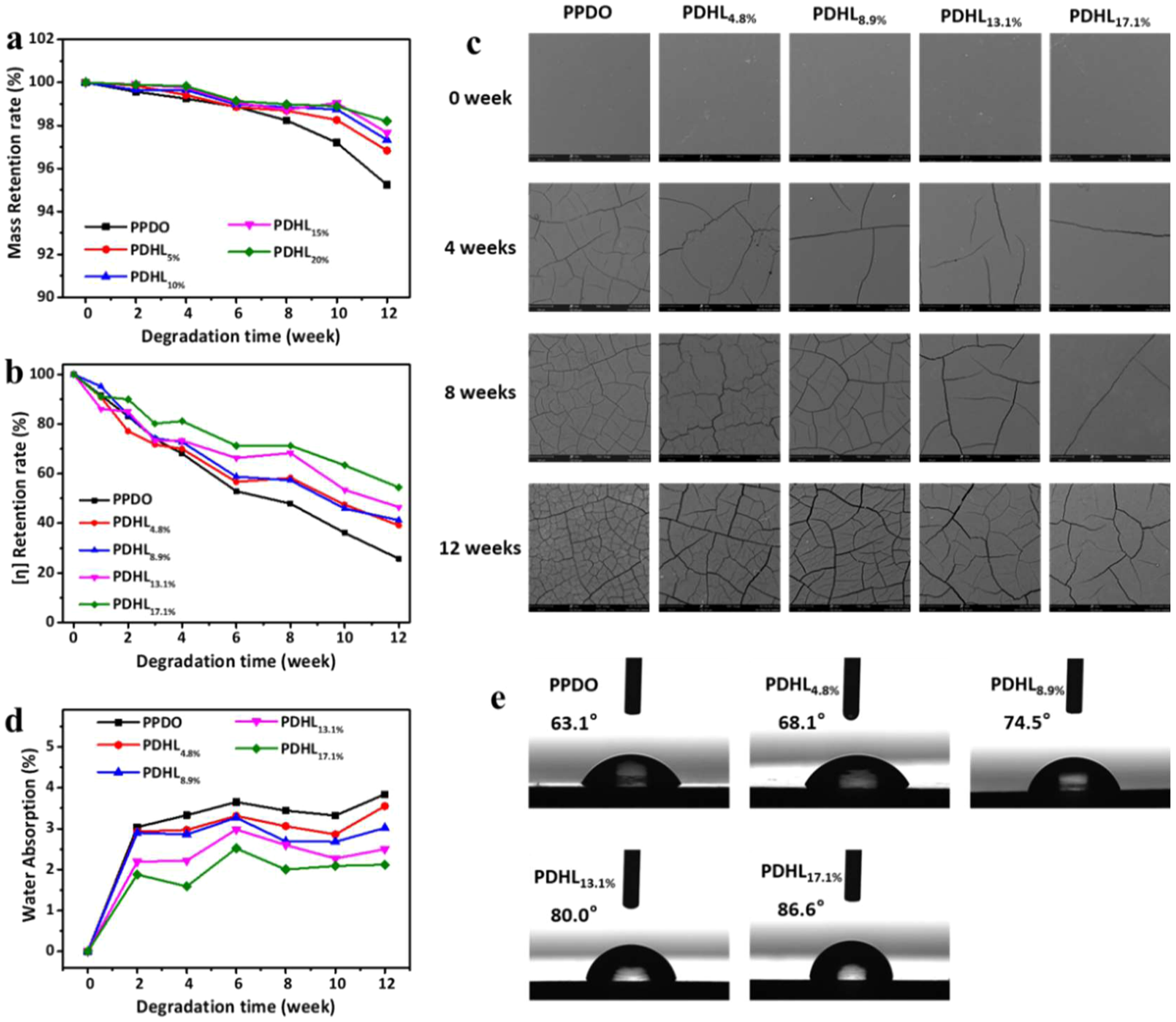

Figure 3. Properties and microstructure changes of the different copolymers and PPDO homopolymers during hydrolytic degradation: (a) mass retention rate, (b) [*η*] retention rate, (c) SEM photographs, and (d) water absorption. (e) WCA of the different copolymers and PPDO homopolymers.

added, the conversion of PDO can also reach 97% (sample PPDO-2). However, in comparison, using DPP as a catalyst can result in a good polymerization efficiency for both PDO and HL at room temperature, corresponding to 93 and 92% of conversion (samples PPDO-4 and PHL-2), respectively, which obviously indicates that the DPP should be very applicable to catalyze the copolymerization of PDO and HL.

Indeed, the copolymerization of PDO and HL with DPP/BDO as catalyst/initiator system at RT can achieve 94 and 92% of the conversion for HL and PDO (sample PDHL-1), respectively. When increasing the temperature, the conversion of PDO and HL decreased (samples PDHL-2 and PDHL-3), whereas using higher boiling point $Ph(CH_2OH)_2$ as the initiator instead of BDO, the conversions of HL and PDO at 80 °C can reach 95 and 94% (sample PDHL-4), respectively, indicating that using the DPP/$Ph(CH_2OH)_2$ as catalytic/initiator system is feasible for synthesizing the PDHL copolymers.

Based on the above results, the homopolymers of PPDO and PHL as well as their copolymers having different compositions were synthesized by bulk ROP with the DPP/$Ph(CH_2OH)_2$ catalytic/initiator system at 80 °C for 36 h (Figure 1a). As shown in Table 1, the conversions of all samples are above 90%. The amounts of HL unit incorporation (mol %) in copolymers calculated by ^1H NMR spectra are ranged from 4.8 to 17.1% with increasing feed amount of HL monomer from 5 to 20%. Furthermore, when the HL molar feed percentages were increased to 40 and 50% (Table S3), the corresponding molar percentage contents of the HL in the copolymers can reach 36 and 50%, respectively. The ^1H NMR spectra of PPDO and PHL homopolymers together with PDHL copolymer are shown in Figure S1, which solidly demonstrates that the copolymerization was realized successfully. The intrinsic viscosity ([*η*]) of PPDO homopolymer and all copolymers is about 1 dg/L. In addition, weight-average molecular weight (M_w) and polymer dispersity index ($Đ$) of

https://doi.org/10.1021/acs.macromol.4c02498
Macromolecules 2025, 58, 4183−4193

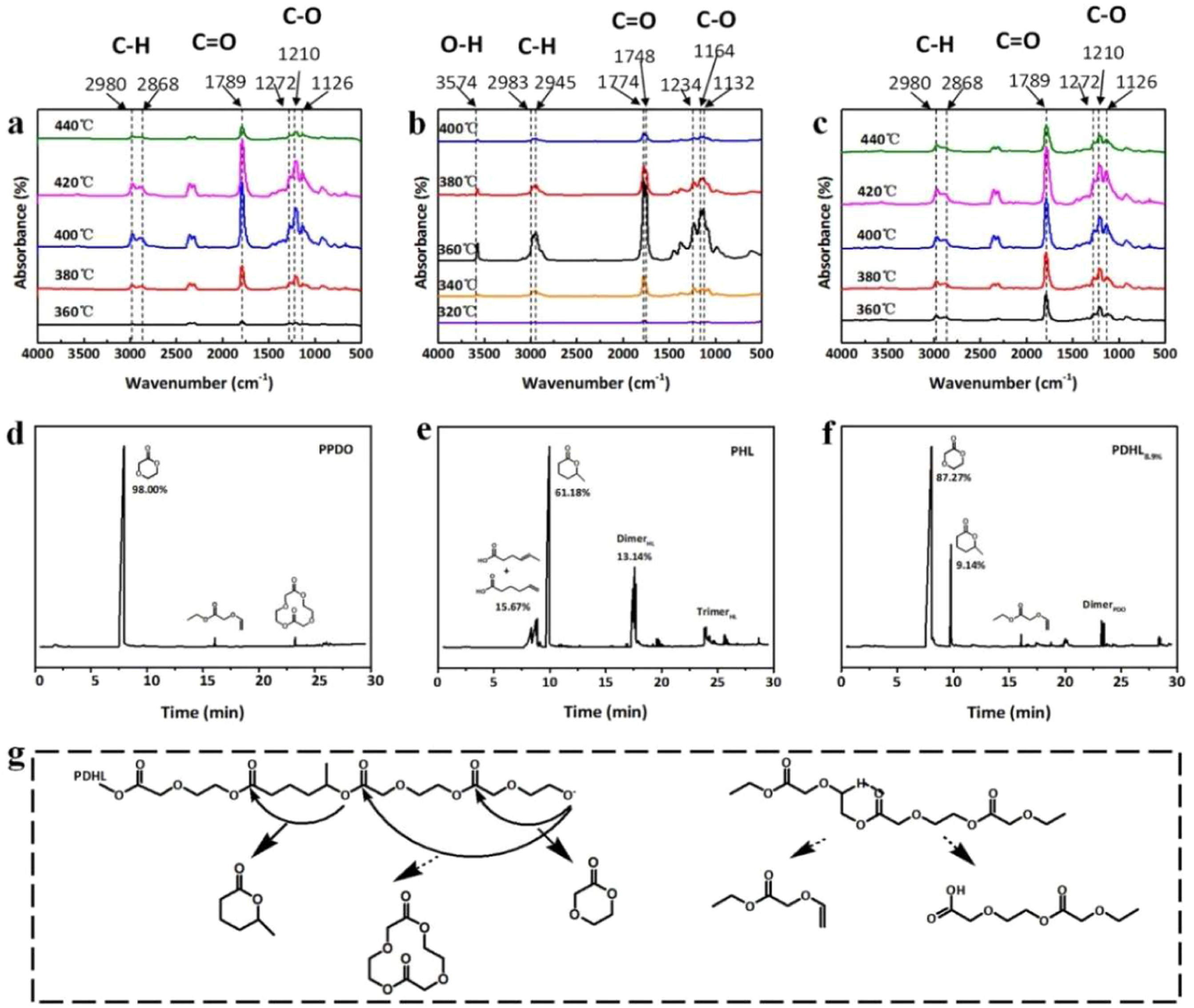

Figure 4. (a–c) FTIR spectra of thermal degradation products from TG-FTIR: (a) PPDO, (b) PHL, and (c) $PDHL_{8.9\%}$. (d–f) Mass spectra analysis of pyrolysis products at 350 °C from Py-GC/MS: (d) PPDO, (e) PHL, and (f) $PDHL_{8.9\%}$. (g) Main thermal degradation route of PDHL copolymer.

Table 3. Chemical Recovery of the Different Copolymers, PPDO, and PHL homopolymers[a]

		NMR		GC
sample	liquid yield[b]	F_{PDHL}[c] (%)	$F_{remonomer}$[d] (%)	purity[e] (%)
PPDO	95	N. A	N. A	99.34
$PDHL_{4.8\%}$	97	4.8	4.5	99.71
$PDHL_{8.9\%}$	96	8.9	9.2	99.80
$PDHL_{13.1\%}$	97	13.1	12.8	99.71
$PDHL_{17.1\%}$	96	17.1	16.3	99.74

[a]The chemical recovery conditions were as follows: 5 g polymer with the presence of $Sn(Oct)_2$, constant temperature at 180 °C, and reduced pressure to 100−300 Pa. [b]The results were obtained by calculating the ratio of the mass of the recovered monomer to the mass of the copolymer before recovery. [c]The molar percentage content of the HL monomer incorporation in copolyester before recovery measured by ^{1}H NMR. [d]The molar percentage content of the HL monomer in the recovery liquid measured by ^{1}H NMR. [e]The percentage content of both HL and PDO in the recovered liquid product measured by gas chromatography.

the as-prepared polymers were investigated by gel permeation chromatography (GPC), and the relevant GPC curves are shown in Figure S2. It can be found that all samples have high molecular weight and their $Đ$ values are in the range of 1.52−1.79 (Table 1), which will guarantee their good comprehensive performance.

In addition, the microstructures of the copolymers were investigated by ^{1}H and ^{13}C NMR. The chemical attribution of different hydrogens in copolymers has been confirmed by ^{1}H NMR spectra, while ^{13}C NMR spectra can provide more detailed information about their microstructure. Taking $PDHL_{50\%}$ copolymer as an example (its structure information is shown in Table S4), for its ^{13}C NMR spectrum (Figures 1b and S3), the signal of the carbonyl carbon of the PDO ring-opened units at near 170 ppm is split into four peaks attributed to different triad sequences,[42] i.e., the sequences of HL−PDO*−PDO, PDO−PDO*−PDO, PDO−PDO*−HL, and HL−PDO*−HL. For the HL ring-opened units, the similar triad sequences can be revealed by ^{13}C NMR spectra, i.e., the sequences of HL−HL*−PDO, PDO−HL*−PDO, HL−

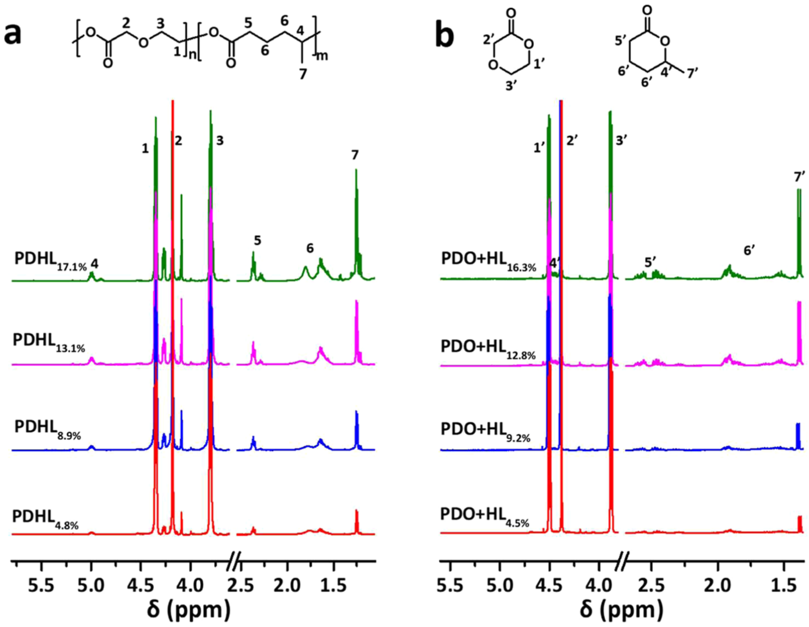

Figure 5. ^{1}H NMR overlays of (a) different copolymers and (b) recovered monomers of the relative copolymers.

Table 4. Comparison of Structure and Properties between PDHL$_{8.9\%}$ and RePDHL$_{9.2\%}$

sample	F_{HL} (%)	M_w (kg/mol)	D	T_m (°C)	ΔH_m (J/g)	T_g (°C)
PDHL$_{8.9\%}$	8.9	56.5	1.75	92.8	51.3	−14.6
RePDHL$_{9.2\%}$	9.2	53.3	1.65	92.9	58.5	−12.8
sample	$T_{5\%}$ (°C)	T_{max} (°C)	elastic modulus (MPa)	yield strength (MPa)	elongation-at-break (%)	
PDHL$_{8.9\%}$	253	369	439.9 ± 11.1	24.7 ± 0.5	240.7 ± 11.5	
RePDHL$_{9.2\%}$	244	386	428.0 ± 2.7	25.0 ± 0.7	227.5 ± 6.4	

HL*−HL, and PDO−HL*−HL. The proportions of sequence structures of copolymers with different HL contents were calculated by ^{13}C NMR spectra. As is well-known, if the probability of an A*−B diad resonance being observed (f_{A*-B}) is equivalent to the product of the multiplication of the mole fractions of monomer A and B ($f_{A*-B,\ theor.} = F_A \times F_B$), the copolymers are deemed as a near-random architecture.[43] By comparing the measured values with the theoretical values calculated from an ideally near-random composition in brackets (Table S5), it is confirmed that the sequence structures of all copolymers are near-random distribution. The near-random structure of the copolymer is related to the trans-esterification at the later stage of the long-term polymerization, which is consistent with the D value obtained by GPC as reported in the prior work.[44]

Thermal Properties, Crystallization Behavior, and Mechanical Properties. The thermal properties of the different copolymers together with PPDO and PHL homopolymers were investigated by thermogravimetric analysis (TGA) and differential scanning calorimetry (DSC) as summarized in Table 2. The TGA curves and DTG curves of the different copolymers together with PPDO and PHL homopolymers are shown in Figure 2a,b. The results show that the initial decomposing temperature (i.e., a temperature corresponding to 5% weight loss, denoted as $T_{5\%}$) and maximum decomposing temperature (T_{max}) of all copolymers are between the values of PPDO and PHL homopolymers. In spite of this, the thermal stability of the copolymers is enough to meet both melt-process and usage.

For all samples, the first heating scans of DSC show the presence of the melting peaks (Figure 2c), indicating their semicrystalline property. The relative melting temperature (T_m) of copolymers between the T_m values of PPDO and PHL decreased from 100.4 to 77.0 °C with increasing the HL content from 4.8 to 17.1 mol %, which is a consequence of the increased disorder along the polymer chains.[43] According to melting enthalpy (ΔH_m) obtained from the first heating scans, the degree of crystallinity (χ_c) was calculated and varied in the range of 40−58% depending on the composition. Compared with PPDO homopolymer (58% of χ_c), the decrease of χ_c for PDHL copolymers is due to the presence of HL units, which hampers the close and order packing of crystalline PPDO chains. However, except for PPDO homopolymer, all PDHL copolymers and PHL homopolymers cannot observe a crystalline peak during the first cooling scans of DSC, further proving the inhibited crystallization of PPDO after HL units are incorporated. Interestingly, for PDHL$_{4.8\%}$ and PDHL$_{8.9\%}$, the cold crystallization peaks and the corresponding melting peaks can be found clearly in the second heating scans of DSC, and the related T_m presents a similarly decreased tendency with increasing the incorporation of HL, while there is almost no cold crystallization and melting for both PHL homopolymer and other copolymers (Figure S4). Furthermore, when the heating and cooling rate of PDHL$_{13.1\%}$ and PDHL$_{17.1\%}$ is slowed down (Figure S5), although there is still no crystallization at a cooling scan, the cold crystallization peaks and corresponding melting peaks can be found in DSC curves of the second heating scans, which indicates that the crystallinity of PDHL$_{13.1\%}$ and PDHL$_{17.1\%}$ copolymers can be

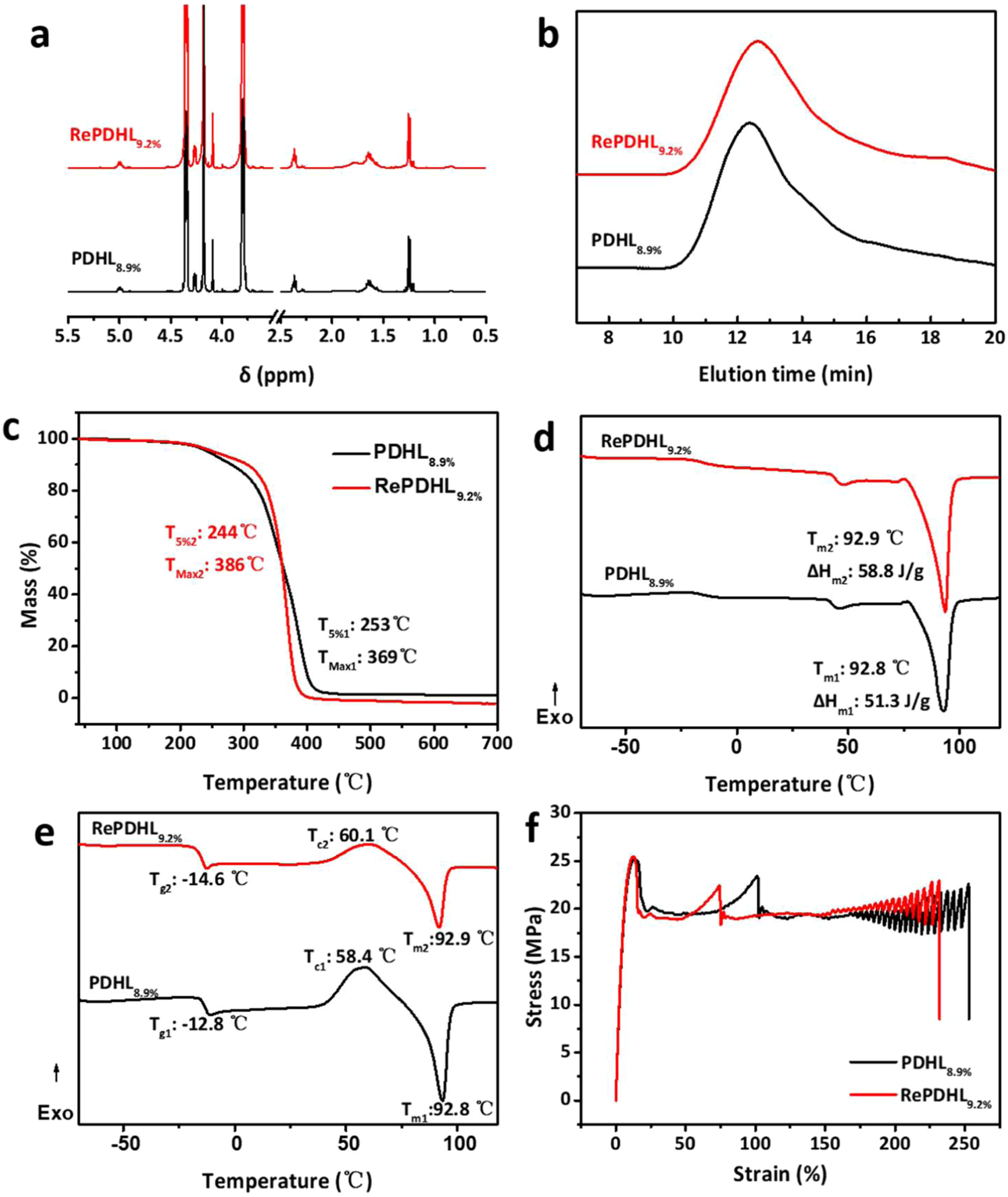

Figure 6. Comparison of $PDHL_{8.9\%}$ copolymer and $RePDHL_{9.2\%}$ copolymer: (a) structure measured by 1H NMR, (b) GPC curves, (c) TGA curves, (d) first heating scans of DSC curves, (e) second heating scans of DSC curves, and (f) stress−strain curves.

recovered if there is enough time. Overall, although the crystallization ability of PDHL copolymers is weaker than that of PPDO, their crystallization can also be completed in enough time and can be controlled by changing the content of HL in the copolymer. In addition, the glass transition temperature (T_g) of copolymer samples with the incorporation of HL units decreases gradually from −8.4 to −15.5 °C, indicating the enhanced chain mobility resulted from the HL units. When the HL content was further increased, a significant decrease in the crystallinity of the copolymer occurred (Figure S6). It can be found from Figure S7 that $PDHL_{36\%}$ is a viscoelastic paste, while $PDHL_{50\%}$ is completely liquid, which does not meet the practical application requirements.

The annealed samples of the different copolymers and homopolymers were characterized by X-ray diffraction analysis (XRD). As shown in Figure 2d, PPDO homopolymer and all copolymers exhibit the same three characteristic semicrystalline diffraction peaks at 2θ of 21.8, 23.6, and 28.9°, while the three diffraction peaks of PHL homopolymer are at 2θ of 17.9, 19.8, and 20.9°. Except PHL homopolymer, the crystallinity (D_c) of other samples calculated by XRD is in the range of 39 to 49%, and the trend of its change for the different copolymers is consistent with the result of DSC, that is the crystallinity decreases with the increase of HL content in copolymers.

The mechanical properties of the PDHL copolymers and PPDO homopolymer were tested by an Instron Universal

Testing machine. The samples having a thickness of approximately 0.5 mm were prepared by melt-pressed process. The testing results are shown in Figure 2e and summarized in Table S6. The stress−strain curves of all samples present a typical feature of thermoplastic materials (Figure S8). It is worth noting that there is ascent first and then descent in some stress−strain curves during elongation of 50−100%, and subsequently, their fluctuation can be seen until fracture. The main reason for the rising and immediate falling of the stress−strain curves could be the stress-induced oriented crystallization that occurs during the unidirectional stretching of the samples and the phenomenon of stress hardening. With regard to the fluctuation, it should be mainly contributed to the yielding and necking in different parts of the sample after stretching to a certain length. Specifically, after elastic deformation, the samples underwent large elongation with small increases in stress, even for the copolymer $\mathrm{PDHL}_{17.1\%}$ with the highest content of HL. In comparison with PPDO homopolymer, elastic modulus and strength of the copolymers are lower and decrease steadily with the increase of HL content due to the worse crystallinity of the copolymers. However, elongation-at-break of copolymers in the range of 80−250% first increases and then decreases with increasing HL content. The increase of the elongation-at-break for $\mathrm{PDHL}_{4.8\%}$ and $\mathrm{PDHL}_{8.9\%}$ could be attributed to the weakened crystallinity and the increased chain flexibility when incorporating a small amount of HL. Further elevating the amount of HL incorporation to 13.1 and 17.1% results in the decrease of the elongation-at-break, which should be attributed to the random sequence of polymers affecting the crystallization properties. It can be seen from the DSC first heating curves that the melting point of the copolymer decreases and the melting peak broadens, indicating that the copolymer is not well crystallized and there are crystallization defects, which make the PDHL elongation-at-break change significantly under the combined effect of molecular weight decrease. Overall, the mechanical properties of the copolymers can be controlled effectively to meet the practical application requirements.

Hydrolytic Degradation. The hydrolytic degradation behavior in pure water at 25 °C of the different copolymers and PPDO homopolymers was studied by monitoring the mass retention rate, intrinsic viscosity ($[\eta]$) retention rate, microstructure, and chemical structure of the samples during degradation. As shown in Figure 3a, the mass retention rates of all samples nearly had no significant difference during 0−6 weeks but reduced obviously in the following 8−12 weeks. In comparison, the decrease of the mass retention rate is fastest for PPDO homopolymers, while it is slowed down for PDHL copolymers, especially the sample with the high content of HL, signifying that the hydrolytic degradation of PPDO is improved by incorporating the HL units. As regards the $[\eta]$ retention rate, it can be found from Figure 3b that not only all samples present a rapidly decreased trend with degradation time but also there is a slower loss of $[\eta]$ for copolymers agreeing with the result of mass retention rate.

Furthermore, the slow weight loss and the fast $[\eta]$ drop disclose that the hydrolytic degradation of PDHL copolymer is a random break of ester bonds recognized as a typical mechanism.[46] The surface microstructure of the samples was observed by scanning electron microscope (SEM). As shown in Figure 3c, surface micro-cracks can be observed and increase with degradation time, presumably being induced by the stress from "further crystallization" and "lamella cleavage". Beyond that, after 12 weeks, the surface of all samples became rougher, indicating that an obvious erosion was underwent. Notably, the increase of the HL content can lead to the retarded microstructural changes, corresponding to the decelerated hydrolytic degradation of copolymers.

The changes in water absorption of PDHL copolymers and PPDO homopolymers during hydrolytic degradation are shown in Figure 3d. For all samples, water absorption increases gradually to no more than 4% with degradation time, which reveals a limited diffusion of water inside the samples matrix. In addition, PPDO homopolymer has the highest water absorption, and water absorption decreases observably with increasing amount of HL incorporation. This phenomenon can be ascribed to the differences of hydrophilicity between homopolymer and copolymers. According to the tests of water contact angle (WCA) as shown in Figure 3e, PPDO has the lowest WCA of 63.1° corresponding to the highest hydrophilicity, and WCAs of copolymers elevate from 68.1 to 86.6° with the increase of HL content from 4.8 to 17.1%, indicating the weakened hydrophilicity of copolymers, which contributes to their retarded hydrolytic degradation.

Chemically Recycling to Monomer and Repolymerization. In order to study the chemical recyclability of the PDHL copolymer, the thermal degradation products of the samples were characterized by thermogravimetry-Fourier transform infrared spectroscopy (TG-FTIR) and pyrolysis-gas chromatograph/mass spectrometry (Py-GC/MS) as shown in Figure 4. In general, cis-elimination reaction and trans-esterification reaction are the two main pyrolysis mechanisms of aliphatic polyester: cis-elimination to produce enoic acid and noncyclic oligomer; trans-esterification to produce cyclic oligomer and monomer.[47] For PPDO homopolymer and $\mathrm{PDHL}_{8.9\%}$ copolymer, FTIR spectra of their evolved gases obtained from the TG-FTIR exhibit some signals at 2980, 2868, 1789, 1272, 1210, and 1126 cm^{-1}, in connection with lactone monomers and nonlinear oligomers (Figure 4a,c). For the PHL homopolymer, a new signal in FTIR spectra of the evolved gases emerges at 3574 cm^{-1}, probably indicating the formation of enoic acid (Figure 4b).

Moreover, the chemical structure and composition of pyrolysis-evolved gases of homopolymers and copolymers were confirmed by Py-GC/MS. The main GC fraction of the pyrolysis products of PPDO is PDO monomer with 98% of proportion (Figure 4d), while aside from HL monomer as the main GC fraction (∼61.2%), the hexenoic acid, HL dimer, and trimer with amount of about 38% can be found in the pyrolysis products of PHL (Figure 4e). Significantly, the main GC fractions of the pyrolysis products of the $\mathrm{PDHL}_{8.9\%}$ are PDO and HL monomers (Figure S9), and no obvious peak of the hexenoic acid emerges, being consistent with the result of TG-FTIR (Figure 4f). In addition, there are no obvious peaks of HL dimer and trimer in the PDHL copolymer, which is related to the near-random structure of the copolymer. PDHL copolymer is much less likely to have sequences of HL−HL−HL units along the backbone just because of the low mol % HL (4.8−17.1%) relative to the PHL homopolymer. The main thermal degradation route of PDHL copolymer is illustrated in Figure 4g. Overall, the pyrolysis depolymerization of PDHL copolymer can high efficiency and selectively obtain both PDO and HL monomers.

In our previous work, we found that depolymerizing PPDO to PDO was more high-efficiency when adding trace $\mathrm{Sn(Oct)_2}$ as a catalyst.[48] Thus, the experiments of chemically recycling to monomers for PPDO and various PDHL were carried out under reduced pressure at 180 °C in the presence of trace $Sn(Oct)_2$. As shown in Table 3 and Figure 5, the yields of the distilled liquid of all samples are in the range of 95−97%, and the composition of the recovered monomers in the distilled liquid is basically consistent with that of the relative copolymer calculated by ^1H NMR. Significantly, gas chromatography shows that the purities of the recovered monomers for all samples reach up to over 99.7%.

In order to verify the closed-loop recycling, the ROP of the recycled monomers was implemented under the same conditions. The amount of the HL incorporation in the repolymerized copolymer, named as $RePDHL_{9.2\%}$, is 9.2%. As shown in Table 4 and Figure 6, the chemical structure and physical performance of $PDHL_{8.9\%}$ and $RePDHL_{9.2\%}$, including thermal stability, thermal properties and tensile properties, are compared. Both the structure and performance of repolymerized copolymer are almost the same as the initial copolymer. All in all, the closed-loop recycling of PDHL copolymer, i.e., polymerization−depolymerization−repolymerization, is well-realized.

■ CONCLUSIONS

In this work, the novel PDHL random copolymers with controlled composition were synthesized successfully by ROP of PDO and HL monomers using DPP as a catalyst. By changing the HL incorporation in copolymers with a mild degree of random in PPDO segments to retain the PPDO advantages, not only can thermal stability, crystallinity, and mechanical properties of PDHL copolymers be adjusted, but also the comprehensive performance has a trade-off that meets the requirements of the practical applications. In addition, when compared with pure PPDO, the introduction of the PHL segment in this PPDO-based copolymer endows with decelerated hydrolysis degradability. By TG-FTIR and Py-GC/MS, the pyrolysis of both copolymer and homopolymers was investigated, and corresponding monomers were found as main pyrolysis products. Accordingly, chemically recycling PDHL copolymers to PDO and HL monomers can be well-performed with high yield and purity. Significantly, as a first sample of a proof-of-concept, the closed-loop recycling of copolymer was realized by repolymerizing two recycled monomers to the PDHL copolymer, having nearly identical structures and properties with the initial copolymer.

■ ASSOCIATED CONTENT

Supporting Information

The Supporting Information is available free of charge at https://pubs.acs.org/doi/10.1021/acs.macromol.4c02498.

Experimental details, characterizations, NMR spectra, GPC curves, stress−strain curves, mass spectrum analysis, TGA curves, and DSC curves. (PDF)

■ AUTHOR INFORMATION

Corresponding Authors

Gang Wu − *The Collaborative Innovation Center for Eco-Friendly and Fire-Safety Polymeric Materials (MoE), National Engineering Laboratory of Eco-Friendly Polymeric Materials (Sichuan), State Key Laboratory of Advanced Polymeric Materials, College of Chemistry, Sichuan University, Chengdu 610064, China;* orcid.org/0000-0002-8306-2076; Email: gangwu@scu.edu.cn

Yu-Zhong Wang − *The Collaborative Innovation Center for Eco-Friendly and Fire-Safety Polymeric Materials (MoE), National Engineering Laboratory of Eco-Friendly Polymeric Materials (Sichuan), State Key Laboratory of Advanced Polymeric Materials, College of Chemistry, Sichuan University, Chengdu 610064, China;* orcid.org/0009-0003-0033-3112; Email: yzwang@scu.edu.cn

Authors

Zheng-He Yang − *The Collaborative Innovation Center for Eco-Friendly and Fire-Safety Polymeric Materials (MoE), National Engineering Laboratory of Eco-Friendly Polymeric Materials (Sichuan), State Key Laboratory of Advanced Polymeric Materials, College of Chemistry, Sichuan University, Chengdu 610064, China;* orcid.org/0000-0002-0457-3880

Xue-Ping Ou-Yang − *The Collaborative Innovation Center for Eco-Friendly and Fire-Safety Polymeric Materials (MoE), National Engineering Laboratory of Eco-Friendly Polymeric Materials (Sichuan), State Key Laboratory of Advanced Polymeric Materials, College of Chemistry, Sichuan University, Chengdu 610064, China*

Si-Chong Chen − *The Collaborative Innovation Center for Eco-Friendly and Fire-Safety Polymeric Materials (MoE), National Engineering Laboratory of Eco-Friendly Polymeric Materials (Sichuan), State Key Laboratory of Advanced Polymeric Materials, College of Chemistry, Sichuan University, Chengdu 610064, China;* orcid.org/0000-0001-9230-0892

Complete contact information is available at: https://pubs.acs.org/10.1021/acs.macromol.4c02498

Author Contributions

[†]Z.-H.Y. and X.-P.O.-Y. contributed equally to this work.

Notes

The authors declare no competing financial interest.

■ ACKNOWLEDGMENTS

This work was supported by the National Key R&D Program of China (2021YFB3801901), the National Natural Science Foundation of China (U19A2095), Institutional Research Fund from Sichuan University (2020SCUNL205), the Fundamental Research Funds for the Central Universities, and the Higher Education Discipline Innovation Project (B20001).

■ REFERENCES

(1) Brahney, J.; Hallerud, M.; Heim, E.; Hahnenbergeret, M.; Sukumaran, S. Plastic rain in protected areas of the United States. *Science* **2020**, *368*, 1257−1260.

(2) Rochman, C. M.; Browne, M. A.; Halpern, B. S.; Hentschel, B. T.; Hoh, E.; Karapanagioti, H. K.; Rios-Mendoza, L. M.; Takada, H.; Teh, S.; Thompson, R. C. Classify plastic waste as hazardous. *Nature* **2013**, *494*, 169−171.

(3) Vethaak, A. D.; Legler, J. Microplastics and human health. *Science* **2021**, *371*, 61−65.

(4) MacLeod, M.; Arp, H. P. H.; Tekman, M. B.; Jahnke, A. The global threat from plastic pollution. *Science* **2021**, *373*, 61−65.

(5) Revell, L. E.; Kuma, P.; Le Ru, E. C.; Somerville, W. R. C.; Gaw, S. Direct radiative effects of airborne microplastics. *Nature* **2021**, *598*, 462−467.

(6) Zhu, Y.; Romain, C.; Williams, C. K. Sustainable polymers from renewable resources. *Nature* **2016**, *540*, 354−362.

(7) Sathe, D.; Zhou, J.; Chen, H.; Su, H.-W.; Xie, W.; Hsu, T.-G.; Schrage, B. R.; Smith, T.; Ziegler, C. J.; Wang, J. Olefin metathesis-based chemically recyclable polymers enabled by fused-ring monomers. *Nat. Chem.* **2021**, *13*, 743−750.

(8) Sun, Y.; An, Z.; Gao, Y.; Hu, R.; Liu, Y.; Lu, H.; Lu, X. B.; Pang, X.; Qin, A.; Shen, Y.; et al. New sustainable polymers with on-demand depolymerization property. *Sci. China Chem.* **2024**, *67*, 2803−2841.

(9) Li, Z.; Shen, Y.; Li, Z. Ring-Opening Polymerization of Lactones to Prepare Closed-Loop Recyclable Polyesters. *Macromolecules* **2024**, *57*, 1919−1940.

(10) Law, K. L.; Narayan, R. Reducing environmental plastic pollution by designing polymer materials for managed end-of-life. *Nat. Rev. Mater.* **2022**, *7*, 104−116.

(11) Haider, T. P.; Völker, C.; Kramm, J.; Landfester, K.; Wurm, F. R. Plastics of the future? The impact of biodegradable polymers on the environment and on society. *Angew. Chem., Int. Ed.* **2019**, *58*, 50−62.

(12) Ragaert, K.; Delva, L.; van Geem, K. Mechanical and chemical recycling of solid plastic waste. *Waste Manage.* **2017**, *69*, 24−58.

(13) Coates, G. W.; Getzler, Y. D. Y. L. Chemical recycling to monomer for an ideal, circular polymer economy. *Nat. Rev. Mater.* **2020**, *5*, 501−516.

(14) Nelson, T. F.; Rothauer, D.; Sander, M.; Mecking, S. Degradable and Recyclable Polyesters from Multiple Chain Length Bio- and Waste-Sourceable Monomers. *Angew. Chem., Int. Ed.* **2023**, *62*, No. e202310729.

(15) Shieh, P.; Zhang, W.; Husted, K. E. L.; Kristufek, S. L.; Xiong, B.; Lundberg, D. J.; Lem, J.; Veysset, D.; Sun, Y.; Nelson, K. A.; Plata, D. L.; Johnson, J. A. Cleavable comonomers enable degradable, recyclable thermoset plastics. *Nature* **2020**, *583*, 542−547.

(16) Liu, Y.; Zhou, H.; Guo, J. Z.; Ren, W. M.; Lu, X. B. Completely recyclable monomers and polycarbonate: approach to sustainable polymers. *Angew. Chem., Int. Ed.* **2017**, *56*, 4862−4866.

(17) Shi, C.; Diment, W. T.; Chen, E. Y.-X. Closed-Loop Recycling of Mixed Plastics of Polyester and CO_2-Based Polycarbonate to a Single Monomer. *Angew. Chem., Int. Ed.* **2024**, *63*, No. e202405083.

(18) Cederholm, L.; Olsén, P.; Hakkarainen, M.; Odelius, K. Design for Recycling: Polyester- and Polycarbonate-Based A-B-A Block Copolymers and Their Recyclability Back to Monomers. *Macromolecules* **2023**, *56*, 3641−3649.

(19) Hong, M.; Chen, E. Y.-X. Completely recyclable biopolymers with linear and cyclic topologies via ring-opening polymerization of gamma-butyrolactone. *Nat. Chem.* **2016**, *8*, 42−49.

(20) Zhang, X.; Guo, W.; Zhang, C.; Zhang, X. A recyclable polyester library from reversible alternating copolymerization of aldehyde and cyclic anhydride. *Nat. Commun.* **2023**, *14*, No. 5423.

(21) Zhu, J.-B.; Chen, E. Y.-X. Living coordination polymerization of a six-five bicyclic lactone to produce completely recyclable polyester. *Angew. Chem., Int. Ed.* **2018**, *57*, 12558−12562.

(22) Zhu, J.-B.; Watson, E. M.; Tang, J.; Chen, E. Y.-X. A synthetic polymer system with repeatable chemical recyclability. *Science* **2018**, *360*, 398−403.

(23) Fahnhorst, G. W.; Hoye, T. R. A Carbomethoxylated Polyvalerolactone from Malic Acid: Synthesis and Divergent Chemical Recycling. *ACS Macro Lett.* **2018**, *7*, 143−147.

(24) Sangroniz, A.; Zhu, J.-B.; Tang, X.; Etxeberria, A.; Chen, E. Y.-X.; Sardon, H. Packaging materials with desired mechanical and barrier properties and full chemical recyclability. *Nat. Commun.* **2019**, *10*, No. 3559.

(25) Shi, C.; Li, Z.-C.; Caporaso, L.; Cavallo, L.; Falivene, L.; Chen, E. Y.-X. Hybrid monomer design for unifying conflicting polymerizability, recyclability, and performance properties. *Angew. Chem., Int. Ed.* **2023**, *62*, 670−685.

(26) Ma, K.; An, H.-Y.; Nam, J.; Reilly, L. T.; Zhang, Y.-L.; Chen, E. Y.-X.; Xu, T.-Q. Fully recyclable and tough thermoplastic elastomers from simple bio-sourced δ-valerolactones. *Nat. Commun.* **2024**, *15*, No. 7904.

(27) Dainton, F. S.; Ivin, K. J. Reversibility of the Propagation Reaction in Polymerization Processes and its Manifestation in the Phenomenon of a 'Ceiling Temperature'. *Nature* **1948**, *162*, 705−707.

(28) Olsén, P.; Odelius, K.; Albertsson, A. C. Thermodynamic Presynthetic Considerations for Ring-Opening Polymerization. *Biomacromolecules* **2016**, *17*, 699−709.

(29) Yuan, P. J.; Hong, M. Ring-opening Polymerizations of the ″Non-strained″ γ-Butyrolactone and Its Derivatives: An Overview and Outlook. *Acta Polym. Sin.* **2019**, *50*, 327−337.

(30) Yang, K. K.; Wang, X. L.; Wang, Y. Z. Poly(p-dioxanone) and its copolymers. *J. Macromol. Sci.* **2002**, *42*, 373−398.

(31) Chen, X. S.; Chen, G. Q.; Tao, Y. H.; Wang, Y. Z.; Lv, X. B.; Zhang, L. Q.; Zhu, J.; Zhang, J.; Wang, X. H. Research Progress in Eco-polymers. *Acta Polym. Sin.* **2019**, *50*, 1068−1082.

(32) Wu, G.; Chen, S.; Liu, C.; Wang, Y. Direct Aqueous Self-Assembly of an Amphiphilic Diblock Copolymer toward Multistimuli-Responsive Fluorescent Anisotropic Micelles. *ACS Nano* **2015**, *9*, 4649−4659.

(33) Wu, G.; Wang, Z.; Bai, Q. Simultaneous Dual Thermoresponsiveness and Fluorescence of Degradable Amphiphilic Diblock Copolymers in Water: Synergy of Supramolecular Interactions and Crystallization. *Macromolecules* **2019**, *52*, 5907−5916.

(34) Wu, G.; Chen, S. C.; Zhan, Q.; Wang, Y. Z. Well-Defined Amphiphilic Biodegradable Comb-Like Graft Copolymers: Their Unique Architecture-Determined LCST and UCST Thermoresponsivity. *Macromolecules* **2011**, *44*, 999−1008.

(35) Liu, C. L.; Wu, G.; Chen, S. C.; You, J.; Wang, Y. Z. Crystallization induced micellization of poly(p-dioxanone)-block-polyethylene glycol diblock copolymer functionalized with pyrene moiety. *Chin. Chem. Lett.* **2014**, *25*, 1311−1317.

(36) Pillai, C. K. S.; Sharma, C. P. Review Paper: Absorbable Polymeric Surgical Sutures: Chemistry, Production, Properties, Biodegradability, and Performance. *J. Biomater. Appl.* **2010**, *25*, 291−366.

(37) Song, C. X.; Cui, X. M.; Schindler, A. Biodegradable copolymers based on p-dioxanone for medical application. *Med. Biol. Eng. Comput.* **1993**, *31*, S147−S151.

(38) Yan, Y. T.; Wu, G.; Chen, S. C.; Wang, Y. Z. Controlled synthesis and closed-loop chemical recycling of biodegradable copolymers with composition-dependent properties. *Sci. China Chem.* **2022**, *65*, 943−953.

(39) Xiong, W. T.; Wu, G.; Chen, S. C.; Wang, Y. Z. Chemically recyclable copolyesters from bio-renewable monomers: controlled synthesis and composition-dependent applicable properties. *Sci. China Chem.* **2023**, *66*, 2062−2069.

(40) Chaos, A.; Sangroniz, A.; Gonzalez, A.; Iriarte, M.; Sarasue, J. R.; Ríoc, J. D.; Etxeberria, A. Tributyl citrate as effective plasticizer for biodegradable polymers: effect of plasticizer on free volume and transport and mechanical properties. *Polym. Int.* **2019**, *68*, 125−133.

(41) Schneiderman, D. K.; Hillmyer, M. A. Aliphatic Polyester Block Polymer Design. *Macromolecules* **2016**, *49*, 2419−2428.

(42) Hong, M.; Tang, X.; Newell, B. S.; Chen, E. Y.-X. "Nonstrained" γ-Butyrolactone-Based Copolyesters: Copolymerization Characteristics and Composition-Dependent (Thermal, Eutectic, Cocrystallization, and Degradation) Properties. *Macromolecules* **2017**, *50*, 8469−8479.

(43) Wilson, J. A.; Hopkins, S. A.; Wright, P. M.; Dove, A. P. Synthesis of ω-Pentadecalactone Copolymers with Independently Tunable Thermal and Degradation Behavior. *Macromolecules* **2015**, *48*, 950−958.

(44) Yang, Z. H.; Tian, G. Q.; Chen, S. C.; Wu, G.; Wang, Y. Z. Regulating Properties of Poly(p-dioxanone) Enabled by Introducing n-Alkyl Substituents of δ-Lactone. *Acta Polym. Sin.* **2022**, *53*, 236−244.

(45) Ishikiriyama, K.; Pyda, M.; Zhang, G. E.; Forschner, T.; Grebowicz, J.; Wunderlich, B. Heat capacity of poly-p-dioxanone. *J. Macromol. Sci., Part B* **1998**, *37*, 27−44.

(46) Chen, S. C.; Wang, X. L.; Wang, Y. Z.; Yang, K. K.; Zhou, Z. X.; Wu, G. In vitro degradation of biodegradable blending materials based

on poly(p-dioxanone) and poly(vinyl alcohol)-graft-poly(p-dioxanone) with high molecular weights. *J. Biomed. Mater. Res., Part A* **2007**, *80A*, 453−465.

(47) Nishida, H.; Yamashita, M.; Hattori, N.; Endo, T.; Tokiwa, Y. Thermal decomposition of poly(1,4-dioxan-2-one). *Polym. Degrad. Stab.* **2000**, *70*, 485−496.

(48) Li, X. Y.; Zhou, Q.; Wen, Z. B.; Hui, Y.; Yang, K. K.; Wang, Y. Z. Influence of catalysts used in synthesis of poly(p-dioxanone) on its thermal degradation behaviors. *Polym. Degrad. Stab.* **2015**, *121*, 253−260.